Shahrood University of Technology

Iranian Society of Mining Engineering (IRSME)

**Journal of Mining and Environment (JME)**

**journal homepage: www.jme.shahroodut.ac.ir**

THOMSON REUTERS

# Reliability Analysis of Surface Settlement caused by Mechanized Tunneling-a Case Study

Hadi Fattahi* and Fateme Jiryaee

*Faculty of Earth Sciences Engineering, Arak University of Technology, Arak, Iran.*

## Article Info

*Received 13 January 2022*

*Received in Revised form 14 February 2022*

*Accepted 20 February 2022*

*Published online 20 February 2022*

*DOI:10.22044/jme.2022.11570.2143*

## Keywords

*Surface settlement*

*Mechanized tunneling*

*Reliability methods*

*GMDH neural network*

*Genetic algorithm*

## Abstract

The surface settlement is an essential parameter in the operation of mechanized tunneling that should be determined before excavation. The surface settlement analysis caused by mechanized tunneling is a geo-technical problem characterized by various sources of uncertainty. Unlike the deterministic methods, the reliability analysis can take into account the uncertainties for the surface settlement assessment. In this work, the reliability analysis methods (second-order reliability method (SORM), Monte Carlo simulation (MCS), and first-order reliability method (FORM)) based on the genetic algorithm (GA) are utilized to build models for the reliability analysis of the surface settlement. Specifically, for large-scale projects, the limit state function (LSF) is non-linear and hard to apply based on the reliability methods. In order to resolve this problem, the GMDH (group method of data handling) neural network can estimate LSF without the need for additional assumptions about the function form. In this work, the GMDH neural network is adapted to obtain LSF. In the GMDH neural network, the tail void grouting pressure, groundwater level from tunnel invert, depth, average penetrate rate, distance from shaft, pitching angle, average face pressure, and percent tail void grout filling are used as the input parameters. At the same time, the surface settlement is the output parameter. The field data from the Bangkok subway is used in order to illustrate the capabilities of the proposed reliability methods.

## 1. Introduction

The surface settlement, particularly in big cities, is one of the most dangerous parameters in the subways and other excavations [1,2]. The ground settlements due to the construction of tunnels can cause a significant damage to the buildings (see Figure 1). Thus before the excavation, a theoretical prediction of the surface settlement is often conducted. Any tunnel eventually disturbs the initial stress field, which contributes to the settlement. The ground motions may be broad enough to disturb the neighboring structures. In urban areas, it is necessary to protect the existing buildings from the problems caused by tunneling [3]. Efforts have been made in the recent decades in order to develop some solutions for settlement caused by tunneling. For example, Atkinson, Potts [4] have studied the effect of the burial depth on the surface settlement above shallow excavations driven in the sand and clay. Hamza et al. [5] have presented a methodology for estimation of the surface settlement in the Cairo Metro. Chi et al. [6] have proposed empirical relations in order to forecast the tunneling-induced ground movement in the silty sand and silty clay. In the study of analytical solutions, Chou, Bobet [7] have utilized some tunnels in order to assess estimations for shallow tunnels in the saturated soil from a practical explanation. Also for deep and shallow tunnels in clays, Park [8] has employed elastic solutions in order to estimate the tunneling-induced undrained ground movements. Ocak, Seker [9] have applied different methods

Corresponding author: H.fattahi@arakut.ac.ir (H. Fattahi).

including the Gaussian processes (GP), support vector machines (SVM), and artificial neural network (ANN) to predict settlement due to tunnel construction. Mohammadi et al. [10] have employed multiple regression and ANN to estimate surface settlement in a subway tunnel in Iran. Hasanipanah et al. [1] have presented a hybrid model of ANN improved by particle swarm optimization (PSO) to estimate maximum settlement due to tunnel construction. Pourtaghi, Lotfollahi-Yaghin [3] have proposed a method of settlement estimation, which is based on coupling ANN and wavelet (Wavenet). Neaupane, Adhikari [11] have presented a way to estimate ground movement around tunnels with the help of input parameters, horizontal ground movement, and surface settlement. Yao et al. [12] have presented a model based on SVM for estimation of the tunnel surrounding rock displacement. Wang et al. [13] have suggested a deformation estimation model based on the least square SVM, genetic algorithm, and Markova theory. Santos Jr, Celestino [14] have developed an ANN model for the prediction of surface settlement in the São Paulo subway. Suwansawat, Einstein [15] have proposed an ANN model to forecast the settlement caused by mechanized tunneling. Xu, Xu [16] have presented the grey correlation methods to calculate the possibility of metro-caused soil settlement. With the development of numerical methods and computer hardware, the finite element (FE) is a common technique used for estimation of surface settlement due to a tunnel construction [17]. In using tunneling simulation, FE can often compute any stress redistributions and deformations without constructing real tunnels [3]. Limitations of numerical approaches lie in the absence of uncertainty in the variables including support structure parameters and rock/soil strength [18]. In this paper, in order to address the above limitations, the probabilistic methods were developed for reliability analysis of settlement induced by mechanized tunneling. Also with the computational intelligence development, the methods employed to estimate the limit state function (LSF) and compute the failure probability ($P_F$) in reliability approaches include the first-order reliability method (FORM), response surface method, Monte Carlo simulation (MCS), second-order reliability method (SORM), etc [19-23].

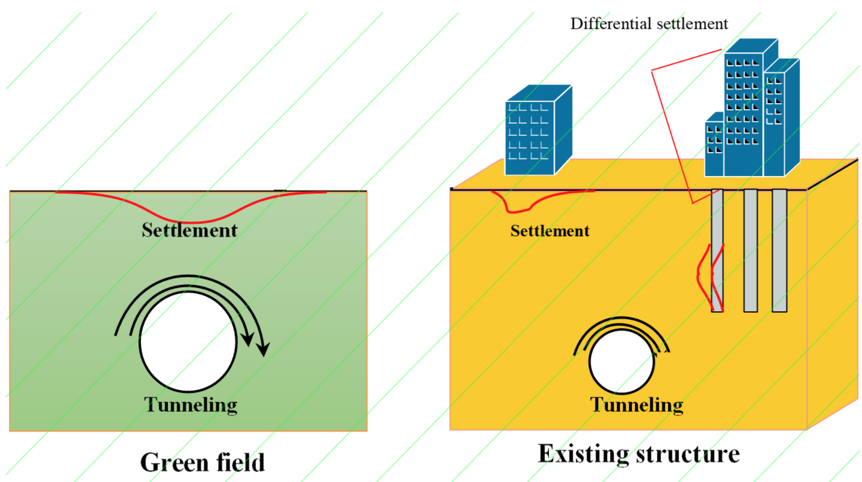


**Figure 1. Ground settlement due to tunnel construction.**

In this work, a new methodology that combines the merits of the genetic algorithm (GA) and GMDH (group data handling method) neural network-based FORM, SORM, and MCS methods for reliability analysis of surface settlement caused by mechanized tunneling are proposed. In this research work, the GMDH neural network is used to approximate LSF without more assumption of the function form. The field data from the Bangkok subway project in Thailand is used to illustrate the capabilities of the reliability methods.

## 2. Basic Theory

Several techniques applied in this paper include the GMDH neural network, GA, and reliability methods (FORM, SORM, and MCS). A brief overview of these techniques is presented here.

### 2.1. Reliability methods
#### 2.1.1. FORM and SORM

The reliability issues are commonly defined by LSF (*g(x)*). $X = \left(X_1, X_2, ..., X_n\right)$ is a random vector that include the simple random parameters that describe loads, rock/soil properties, geometrical quantities, etc. The function $g\left(x\right)$ is laid down as follows:

$$g\left(x\right) = \begin{cases} > 0 \; for\; the\; safe\; state \\ < 0 \; for\; the\; failure\; state \end{cases} \tag{1}$$

The hyperplane $g\left(x\right) = 0$ is named LSF. The function can be written as follows (in the settlement analysis):

$$g\left(x\right) = u_{\max} - U\left(X_1, X_2, ..., X_n\right) \tag{2}$$

where $U$ is the surface settlement of a given point induced by a collection of arbitrary parameters $X_1, X_2, ..., X_n$ such as the subsoil/rock model parameters, geometrical properties, and loads, and $u_{max}$ stands for a maximal permissible settlement. In this case, $g\left(x\right) < 0$ (failure) means the excess of the $u_{max}$ specified. $P_F$ is utilized in the following equation:

$$p_F = \int_{\{g(x)<0\}} f_x(x)dx \,. \tag{3}$$

where $f_x$ indicates a multi-dimensional joint PDF (probability density function). In the special case, if $X$ (random vector) is a Gaussian random vector, a coordinate system transformation is defined as the standardization:

$$y_i = \frac{x_i - E\left(X_i\right)}{\sigma_{Xi}}, \; i = 1, ..., n. \tag{4}$$

where $E\left(X_i\right)$ is the expected value of $X_i$ and $\sigma_{Xi}$ is the standard deviation. Mapping the LSF $g\left(x\right) = 0$ accordingly is as follows:

$$G(y) \equiv g(x(y)) = 0 \tag{5}$$

$$p_F = \int_{\{G(y)<0\}} \phi_0(y)dy = \Phi_0(-\beta), \tag{6}$$

where $\Phi_0$ is the one-dimensional standard Gaussian probability cumulative function (PCF), $\beta$ is the hyperplane $G(y) = 0$ distance, and $\phi_0$ is the $n$-dimensional standard Gaussian PDF.

The $p_F$ value is hardly reached in the most fundamentally exciting situations, where either non-Gaussian PDFs or non-linear LSFs appear. Then an approximate technique is required to be utilized. Among these techniques, SORM and FORM are most usual in utilizing [24-26]. Some mapping methods of the coordinate system must be used instead of Equation 4. In this mapping, $X$ is changed into the $Y$:

$$Y = Y(X). \tag{7}$$

Therefore, $P_F$ equals:

$$p_F = \int_{\{G(y)<0\}} \phi_0(y)dy \,, \tag{8}$$

In FORM, LSF in the standard normal space is substituted with $\nabla G(y - y^*) = 0$ (tangent hyperplane) at $y^*$ (the so-named *design point*) with the minimum distance from the origin (see Figure 2), and $P_F$ is estimated as:

$$p_F \approx \int_{\{\nabla G(y-y^*)<0\}} \phi_0(y)dy = \Phi_0(-\beta), \tag{9}$$

where $\beta$ is the reliability index and $\Phi_0$ is similar to Eq. (6).

In SORM, LSF is fitted with a quadratic plane in the nearby $y^*$, and the right-hand side of Eq. (9) is multiplied by a factor of certain correction [27], affected by $G(y) = 0$ at $y^*$. Next, by inverting Equation (9), $\beta_{SORM}$ can be calculated by:

$$\beta_{SORM} = -\phi_0^{-1}\left(p_{F\,SORM}\right) \tag{10}$$

The most significant issue in SORM and FORM lies in finding the $y^*$. Therefore, the issue can be described as follows:

$$\begin{aligned} &Minimize \;\; \beta = \|y\|^2 = y^T.y \\ &subject\; to : G(y) = 0 \end{aligned} \tag{11}$$

In this work, GA is utilized to solve the optimization problem.

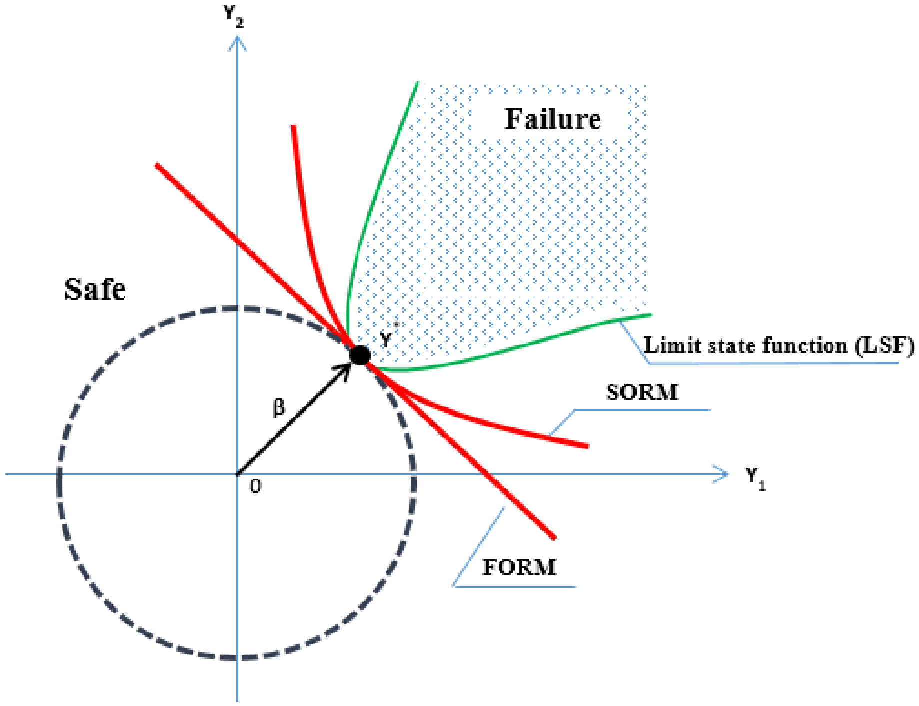


**Figure 2. Schematic performance of SORM and FORM.**

### 2.1.2. MCS

MCS utilizes the randomly created input parameter samples, records the time numbers that failure occurs, and calculates $P_F$ after numerous deterministic analysis repetitions. This technique is easy, simple, and robust to utilize. Thus the method is used in order to evaluate the other methods of analysis. Many papers have been published on the use of MCS (e.g. [28-32]) that how it can be utilized to simulate the issues. In MCS, violation of the limit state is expressed by the condition $g(x_1, x_2, ..., x_n) \le 0$, and $P_F$ is described by the following [33]:

$$P_F = P\left[g(x_1, x_2, ..., x_n) \le 0\right] = \int\int \underset{g(x_1, x_2, ..., x_n) \le 0}{\dots} \int f_{x_1, x_2, ..., x_n}(x_1, x_2, ..., x_n) dx_1 dx_2 ... dx_n \quad (12)$$

where $f_{x_1, x_2, ..., x_n}(x_1, x_2, ..., x_n)$ is the joint PDF, and $(x_1, x_2, ..., x_n)$ is the random variables values.

MCS allows an approximation of PF to be calculated, as follows:

$$P_F = \frac{1}{N} \sum_{i=1}^{N} I(x_1, x_2, ..., x_n) = \frac{N_F}{N} \quad (13)$$

where the total sample number is $N$, the sample number found in the failed state is $N_F$ (see Figure 3), and $I(x_1, x_2, ..., x_n)$ is a function described by:

$$I(x_1, x_2, ..., x_n) = \begin{cases} 1 & if \;\; g(x_1, x_2, ..., x_n) \le 0 \quad Failure\ state \\ 0 & if \;\; g(x_1, x_2, ..., x_n) \rangle\ 0 \quad Safe\ state \end{cases} \quad (14)$$

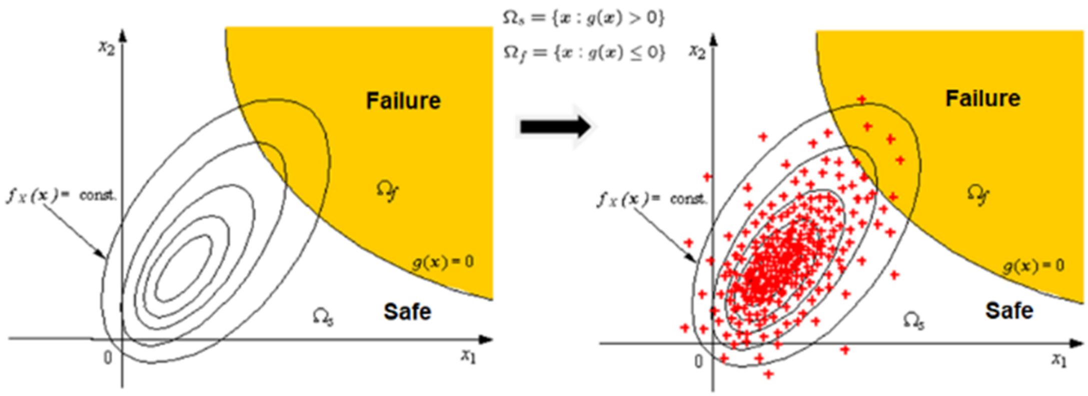


**Figure 3. A schematic presentation of MCS process [32].**

## 2.2. Genetic algorithm for reliability analysis

GA is a stochastic optimization method presented by Holland [34]. GA starts with a randomly created population, and uses three operators in order to find the best solutions: reproduction, mutation, and cross-over [35]. The cross-over combines two chromosome features to create the off-spring. The mutation generates new chromosomes by arbitrarily changing the genes of chromosomes. In a large solution domain, GA is an active algorithm for searching that converges easily to find the best solution.

In this work, the problem in Eq. (11) is non-linear, used by GA in order to solve the optimization problem. GA fundamentally involves three stages:

1. random variables decoding/coding into strings;
2. for each solution, calculating the cost/fitness;
3. using the genetic operators to create a solution string for the next generation.

Based on the reliability index ($\beta$) value, the fitness/cost of each string is calculated. A small $\beta$ value corresponds to a reasonable cost/fitness. Therefore, the fitness/cost function is described as $\frac{1}{\beta}$. The $\beta$ value is penalized if the solution violates the constraints. In GA, the searching process involving the three genetic operators (reproduction, cross-over, and mutation) was replicated, and the cycle continued until:

(1) The $\beta_{averege}$ does not indicate a noticeable change over the former product (γ can be set to 0.95):

$$\beta_{average}^{(k+1)generation} > \gamma\beta_{average}^{k\ generation}$$

(2) The first three separate $\beta_{minimum}$ of the new creation remain the same for the previous creation.

The potential of applying GA for the reliability analysis has been highlighted in many studies. Tun et al. [36] have used GA for the reliability analysis of several slopes. In this work, a GA was developed to solve this optimization problem considering the limit equilibrium approach to search for several failures. Zeng et al. [37] have applied GA and fully specified slip surfaces for the reliability analysis of layered soil slopes. In this work, the Spencer's technique was utilized to calculate the safety factors of trial slip surfaces, and FORM was used to efficiently calculate their reliability. A custom-designed GA was used to search all the representative slip surfaces. Juang, Wang [38] have used multi-objective GA for the reliability-based robust geotechnical design of spread foundations.

## 2.3. GMDH neural network for reliability analysis

LSF can not be directly represented in the reliability analysis of complex engineering problems. As mentioned in the previous section, GA is employed in order to evaluate the reliability of complicated engineering problems, indirectly estimating LSF by the numerical techniques such as the FE process. Limitations of the numerical approaches lie in the absence of uncertainties of factors such as cohesion, friction angle, young's modulus, *in situ* stress, and Poisson's ratio of rock/soil. It is not possible to utilize these methods. In this work, the GMDH neural network is used to approximate LSF.

The GMDH neural network has been proposed by Ivakhnenko [39]. In a wide range of areas such as rock/soil mechanics, the GMDH neural network is utilized for pattern recognition, optimization, and forecasting. A neuron collection created by a second-order polynomial is contained in the GMDH neural network [40]. The network combines neuron-derived second-order polynomials, defines the function $\hat{f}$ with $\hat{y}$ (output) for $x=\{x_1,x_2,x_3,...,x_n\}$ (set of inputs) compared to the measured output (with the least error), and therefore, the $M$ data including one output and $n$ inputs, the actual results are presented as follow:

$$y_i=f\left(x_{i1},x_{i2},x_{i3},...,x_{in}\right) \quad i=1,2,...,M \tag{15}$$

For any given input vector, it is now possible to train the GMDH neural network to estimate $\hat{y}_i$ that is:

$$\hat{y}_i=\hat{f}\left(x_{i1},x_{i2},x_{i3},...,x_{in}\right) \quad i=1,2,...,M \tag{16}$$

The error square between the measured and estimated values should be minimized by the GMDH neural network:

$$\sum_{i=1}^{M}\left[\hat{f}\left(x_{i1},x_{i2},x_{i3},...,x_{in}\right)-y_i\right]^2 \to \min \tag{17}$$

It is possible to define the relation between the output and inputs as follows:

$$y=a_0+\sum_{n}^{1}a_ix_i+\sum_{n}^{1}\sum_{n}^{1}a_{ij}x_ix_j+\sum_{n}^{1}\sum_{n}^{1}\sum_{n}^{1}a_{ijk}x_ix_jx_k+... \tag{18}$$

$$\hat{y}=G\left(x_i,x_j\right)=a_0+a_1x_i+a_2x_j+a_3x_ix_j+a_4x_i^2+a_5x_j^2 \tag{19}$$

By the regression methods, $a_i$ in Eq. (19) is determined so that the difference $y$ (measured) and $\hat{y}$ (predicted) is reduced for $x_i$ and $x_j$ (input variables). The coefficients are achieved for each built neuron (function $G_i$) in order to minimize the overall neuron error. Thus:

$$E=\frac{\sum_{i=1}^{M}\left(y_i-G_i\right)^2}{M} \to \min \tag{20}$$

Double combinations are made from $n$ inputs in the GMDH neural network, and all the neurons coefficients are achieved utilizing the least-squares technique [41]. Thus:

$$\binom{n}{2}=\frac{n\left(n-1\right)}{2} \tag{21}$$

The neurons are built as follows in the second layer:

$$\left\{\left(y_i,x_{ip},x_{iq}\right)\middle|\, i=1,2,...,M \;\&\; p,q\in 1,2,...,M\right\} \tag{22}$$

In the following:

$$Aa=Y \tag{23}$$

where A is the unknown coefficients vector of the quadratic equation presented in Eq. (19).

$$a=\left\{a_0,a_1,a_2,a_3,a_4,a_5\right\} \tag{24}$$

$$Y=\left\{y_1,y_2,y_3,...,y_M\right\}^T \tag{25}$$

The observation is the outputs. Thus:

$$A=\begin{bmatrix} 1 & x_{1p} & x_{1q} & x_{1p}x_{1q} & x_{1p}^2 & x_{1q}^2 \\ 1 & x_{2p} & x_{2q} & x_{2p}x_{2q} & x_{2p}^2 & x_{2q}^2 \\ \cdots & \cdots & \cdots & \cdots & \cdots & \cdots \\ 1 & x_{Mp} & x_{Mq} & x_{Mp}x_{Mq} & x_{Mp}^2 & x_{Mq}^2 \end{bmatrix} \tag{27}$$

The least-squares method of regression method solves the equations as follows:

$$a=\left(A^TA\right)^{-1}A^TY \tag{27}$$

A schematic representation of the suggested GMDH neural network is shown in Figure 4.

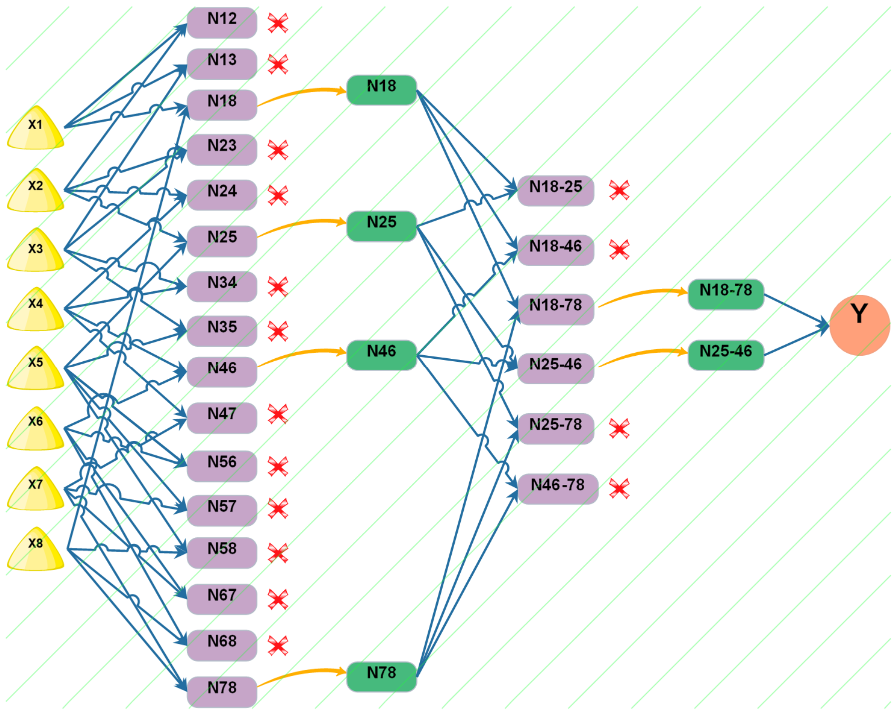


**Figure 4. A schematic representation of the proposed GMDH neural network.**

## 3. Approximate LSF using GMDH Neural Network

### 3.1. Studied area and data

The dataset used in this work was collected from the open source literature [15] in order to evaluate the relationship between the output set and the inputs. The datasets used to generate the database was collected from the Bangkok subway. This project was split into two tunnel parts, namely the south section and the north section. Each dataset contains the variables of pitching angle (PA), geology at tunnel invert, distance from shaft (DS), average penetrate rate (AP), average face pressure (AFP), grouting pressure (G), groundwater level from tunnel invert (Invert to WT) (IWT), geology at tunnel crown, depth (D), grout filling (GF), and measured surface settlement (SS). The descriptive statistics of all datasets are shown in Table 1.

**Table 1 Statistical description of dataset utilized in this paper**

| Parameter | Average | Min | Max |
|---|---|---|---|
| D (m) | 22.05 | 17.89 | 24.82 |
| DS (m) | 1320.27 | 33.60 | 3055.20 |
| IWT (m) | -3.20 | -5.97 | 0.96 |
| AFP (KPa) | 54.73 | 14.50 | 131.00 |
| AP (mm/min) | 42.63 | 20.10 | 76.85 |
| PA (deg) | 0.05 | -1.38 | 1.43 |
| G (bar) | 2.78 | 2.30 | 7.40 |
| GF (%) | 125.96 | 70.00 | 224.00 |
| SS (mm) | -28.09 | -6.25 | -60.5 |

### 3.2. Determining continuous probability distribution of input variables

In the stochastic models, a continuous probability distribution (CPD) was considered for each one of the input variables. In this research work, data processing was performed using the Easy-Fit software in order to find the suited distribution [42]. The Kolmogorov–Smirnov method was utilized to choose the best distributions. As the result of data processing, four best-fitted distributions (gen extreme value, gamma, lognormal and, gen pareto) are shown in Table 2. Furthermore, in order to have a better illustration, the probability distribution functions of the input variables utilized in the reliability analysis are illustrated in Figure 5.

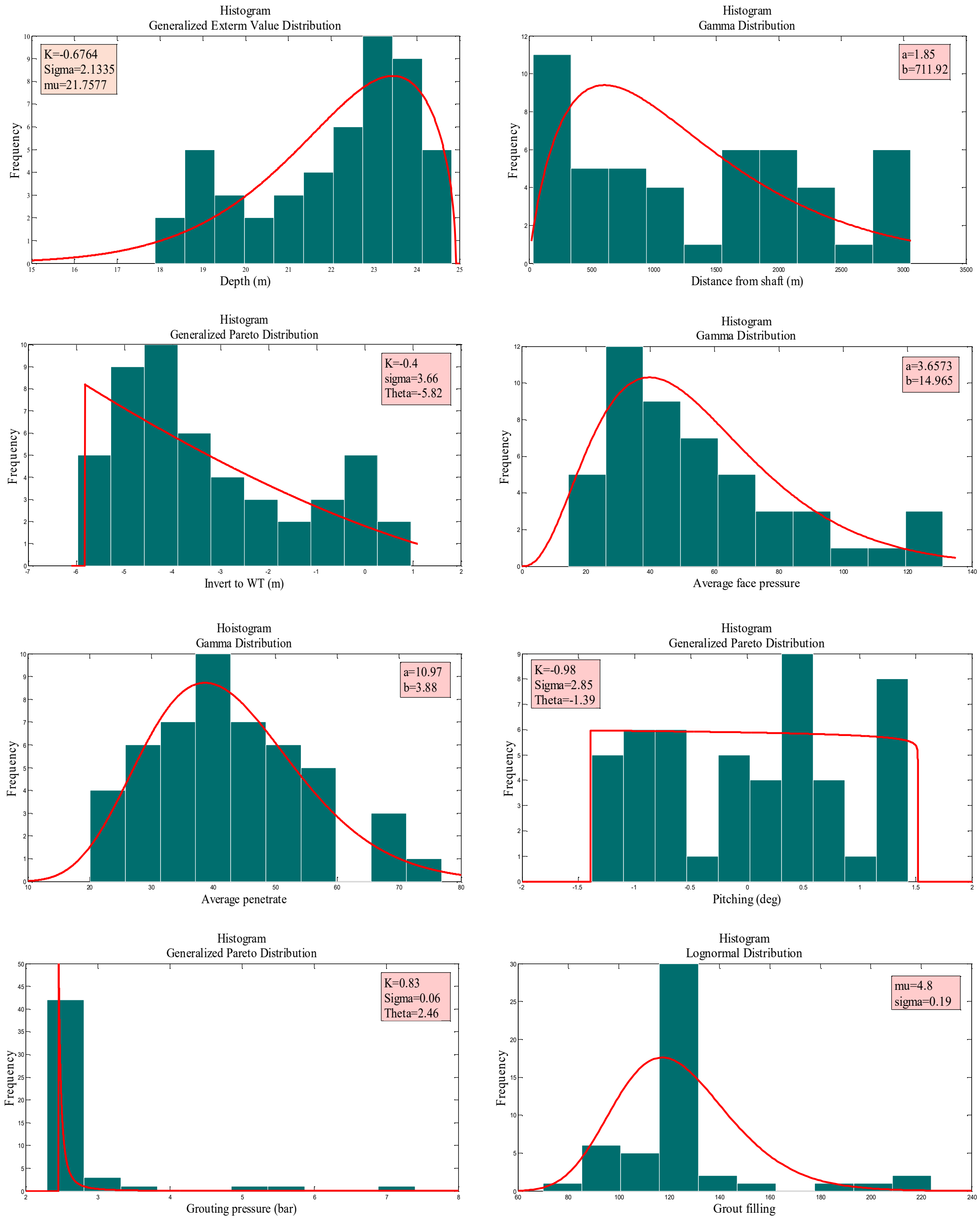


**Figure 5. Continuous probability distribution of input variables used in reliability analysis.**

**Table 2. Continuous probability distribution of input variables.**

| Random variable | Distribution | Parameter (1) | Parameter (2) | Parameter (3) |
|---|---|---|---|---|
| D (m) | Gen extreme value [a] | -0.63 | 2.17 | 21.7 |
| DS (m) | Gamma [b] | 1.85 | 711.92 | - |
| IWT (m) | Gen pareto [a] | -0.4 | 3.66 | -5.82 |
| AFP (KPa) | Gamma | 2.19 | 19.8 | - |
| AP (mm/min) | Gamma | 10.97 | 3.88 | - |
| PA (deg) | Gen pareto | -0.98 | 2.85 | -1.39 |
| G (bar) | Gen pareto | 0.83 | 0.06 | 2.46 |
| GF (%) | Lognormal [c] | 4.8 | 0.19 | - |

[a] Parameters of "gen extreme value" and "gen pareto" distribution are k, σ, and μ.
[b] Parameters of "gamma" distribution are a and b.
[c] Parameters of "lognormal" distribution are μ and σ.

### 3.3. Evaluation of GMDH neural network performance

In order to consider the performances of the GMDH neural network model, the root mean square error (RMSE) and the correlation coefficient ($R^2$) were selected to be the measure of accuracy [43-49]. RMSE and $R^2$ could be described as follows:

$$RMSE=\sqrt{\frac{1}{n}\sum_{k=1}^{n}(t_k-\hat{t}_k)^2} \tag{28}$$

$$R^2=1-\frac{\sum_{k=1}^{n}(t_k-\hat{t}_k)^2}{\sum_{k=1}^{n}t_k^2-\frac{\sum_{i=1}^{n}\hat{t}_k^2}{n}} \tag{29}$$

Let $t_k$ be the measured (actual) value, $\hat{t}_k$ be the estimated value, and $n$ be the observations number.

### 3.4. Explicit formation of approximate LSF

For the reliability analysis, choosing the LSF required in its closed form is preferred. Unfortunately, there is always no closed form. In this work, the GMDH neural network was applied to approximate LSF. Without any expectation of the function form being required, the GMDH neural network strongly resembles the non-linear relationship between the input variables and the surface settlement. Therefore, a professional GMDH neural network program, GMDH Shell, was utilized to run the GMDH neural network. This software does not require the initial data normalization, and noticeably reduce the processing time. The GMDH shell software can provide a separate formula based on the input variables. For an approximate LSF, a data collection containing 49 data points were used, while 39 data points (80%) were used for the approximate LSF, and the remaining data points were used for calculation of the accuracy degree. After modeling, LSF by the software is given by Eq. (30). The variables utilized in the GMDH neural network process is shown in Table 3. Also the measurement of errors (provided by the GMDH shell software) and the comparison of measured with estimated data is presented in Table 4 and Figure 6. Also the correlation between the measured and estimated values of surface settlement is shown in Figure 7.

$$\begin{aligned}
&SS=8.1062+0.6791\times N_{70}+0.6067\times N_{113}\\
&N_{70}=128.3+3.1108\times N_{177}+0.1284\times N_{177}\times N_{183}-0.0284\times N_{177}^2+5.2645\times N_{183}\\
&N_{113}=-304.462-6.4002\times N_{165}-0.0901\times N_{165}\times N_{188}-0.929\times N_{165}^2-16.0016\times N_{188}-0.2508\times N_{188}^2\\
&N_{165}=-36.2374+0.0009\times AFP^2+2.7992\times PA+5.9859\times PA^2\\
&N_{177}=-793.698+54.3713\times D-0.1359\times D\times GF-0.8784\times D^2+2.9849\times GF\\
&N_{183}=-47.6852+0.2739\times G\times GF-3.4884\times G^2-0.0028\times GF^2\\
&N_{188}=-32.7918+0.0144\times DS-0.002\times AP^2
\end{aligned} \tag{30}$$

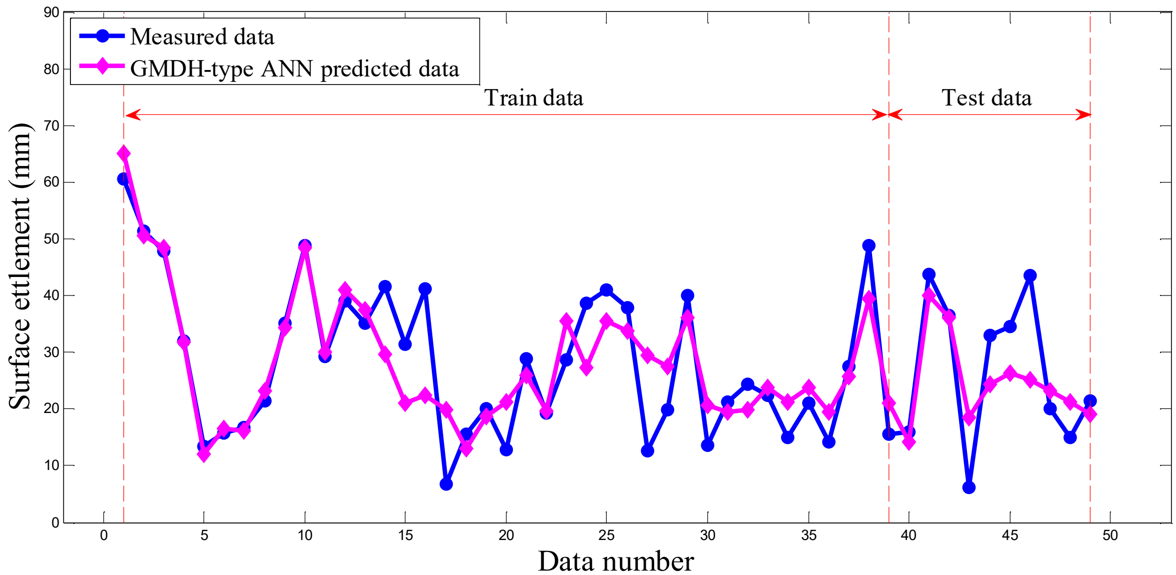


**Figure 6. Comparison of measured values with those of GMDH neural network estimates.**

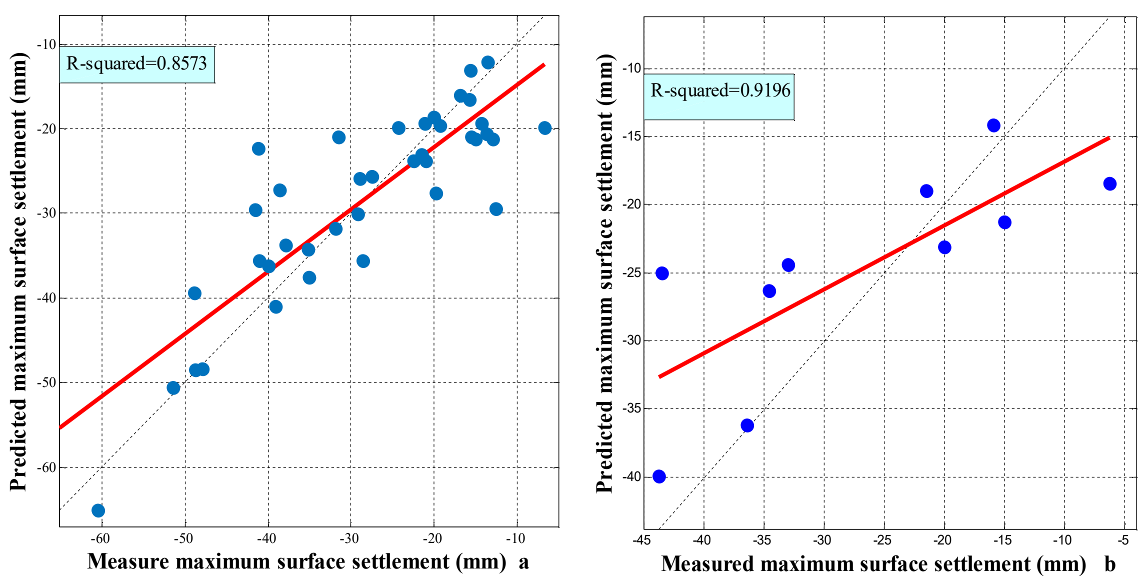


**Figure 7. Correlation between estimated and measured of surface settlement by GMDH neural network (a) training, (b) testing.**

**Table 3. Parameters used in GMDH neural network process.**

| Parameter | Value |
|---|---|
| Core algorithm | GMDH neural network |
| Neuron function | Quadratic polynomial |
| Max number of layers | 3 |
| Number of neurons | 500 |
| Validation strategy | 500 |
| Reorder observation | Odd/even |
| Test data (%) | 20 |

**Table 4. Error measurement by GMDH neural network software.**

| Description | Training | Testing |
|---|---|---|
| Number of observations | 39 | 10 |
| Root mean square error (RMSE) | 6.737 | 8.411 |
| Coefficient of determination ($R^2$) | 0.9535 | 0.9196 |

### 3.5. Analysis of sensitivity

The analysis of sensitivity evaluates the influence of each input variable on the output variable. In this work, the analysis of sensitivity was done using the relevant software. The analysis of sensitivity for the GMDH neural network model is shown in Figure 8. As it can be seen in this figure, the variables PA and GF have maximal effects on the output with 16.92%.

## 4. Reliability analysis of surface settlement caused by mechanized tunneling

After getting LSF in the previous section, GA-FORM, GA-SORM and, MCS (based on GMDH neural network) were used to evaluate the reliability indices $\beta$ and $P_F$ for the surface settlement caused by mechanized tunneling. The flow chart of the reliability analysis procedures (proposed in this work) is shown in Figure 9. It should be noted that based on the limiting settlement ($SS_{limit}$ =50 mm) and Eq. (30), it can be written as $g(x)= SS_{limit} - SS$. In order to verify the accuracy of GA-FORM and GA-SORM, the calculation results are compared with the MCS results; the results of the comparison are shown in Table 5. The calculating procedure was repeated for ten times for each approach listed in Table 5. As presented in Table 5, the reliability indices considered by GA-FORM, GA-SORM, and MCS (based on GMDH neural network) are almost the same, indicating that the proposed GA-FORM and GA-SORM are reliable. Hence, in this paper, the proposed reliability methods can find the best solution of $\beta$ stably whether the performance function is implicit/explicit; however, the computing cost of GA-SORM and GA-FORM is meaningfully less than MCS. The convergence generation numbers are 200 for GA-SORM and GA-FORM. Obviously, GA-SORM and GA-FORM have many merits of efficiency, stability, flexibility and, accuracy, and they can be utilized for the reliability analysis of surface settlement caused by mechanized tunneling. Of course, one should keep in mind that in the reliability analysis of any conditions, MCS can be utilized. [50], and its calculation error is only related to the sample number and its variance [51]. In this work, the upper and lower limits of sample size for surface settlement under different confidence levels were forecasted before MCS simulation. Therefore, the sample size is 600,000, sufficient for an acceptable calculation precision (see Table 6). It should be noted that for GA-FORM and GA-SORM, the GA parameters (see Table 7) are kept constant throughout the whole procedure of reliability analysis, and the converge process of reliability index by GA is illustrated in Figure 10.

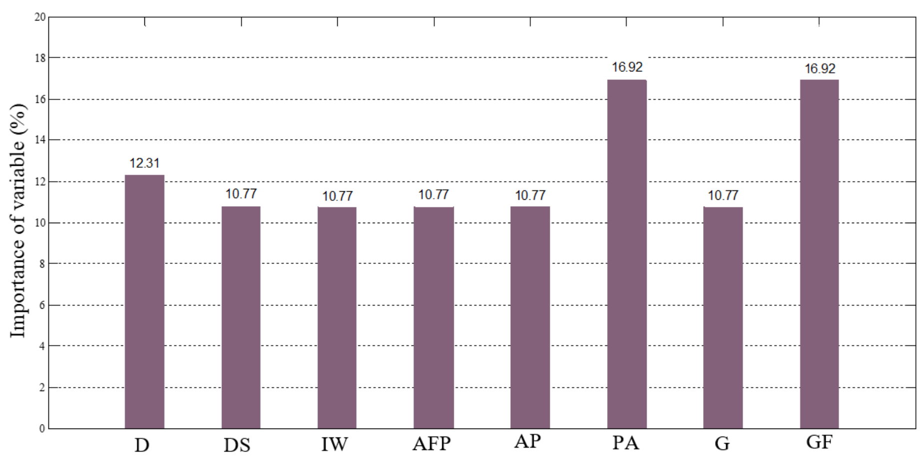


**Figure 8. Relative importance of variables on output in GMDH neural network.**

**Table 5. Results from different reliability methods for surface settlement caused by mechanized tunneling.**

| Method | LSF | Design point | $\beta$[a] | $P_F$[b] | Iteration number |
|---|---|---|---|---|---|
| MCS | GMDH neural network | - | - | 0.0608 | 600,000 |
| GA-FORM | GMDH neural network | [20.56 , 33.60 , -3.36 , 33.76 , | 1.5455 | 0.06113 | 200 |
| GA-SORM | GMDH neural network | 49.69 , -0.31 , 2.49 , 104.05] | 1.5455 | 0.05655 | 200 |

[a] $\beta$ is reliability index.
[b] $P_F$ is probability of failure

**Table 6. $P_F$ for 8 different values of sample size in MCS.**

| Sample size | Probability of failure $P_F$ |
|---|---|
| 100000 | 0.0619 |
| 200000 | 0.0614 |
| 300000 | 0.0613 |
| 400000 | 0.0613 |
| 500000 | 0.0609 |
| 600000 | 0.0608 |
| 700000 | 0.0608 |
| 800000 | 0.0608 |

**Table 7. Parameters used in GA for reliability analysis.**

| Parameter | Value |
|---|---|
| Iterations | 200 |
| Population size | 10000 |
| Cross-over percentage | 0.4 |
| Mutation percentage | 0.95 |
| Gamma | 0.05 |
| Selection pressure | 8 |
| Mutation rate | 0.1 |

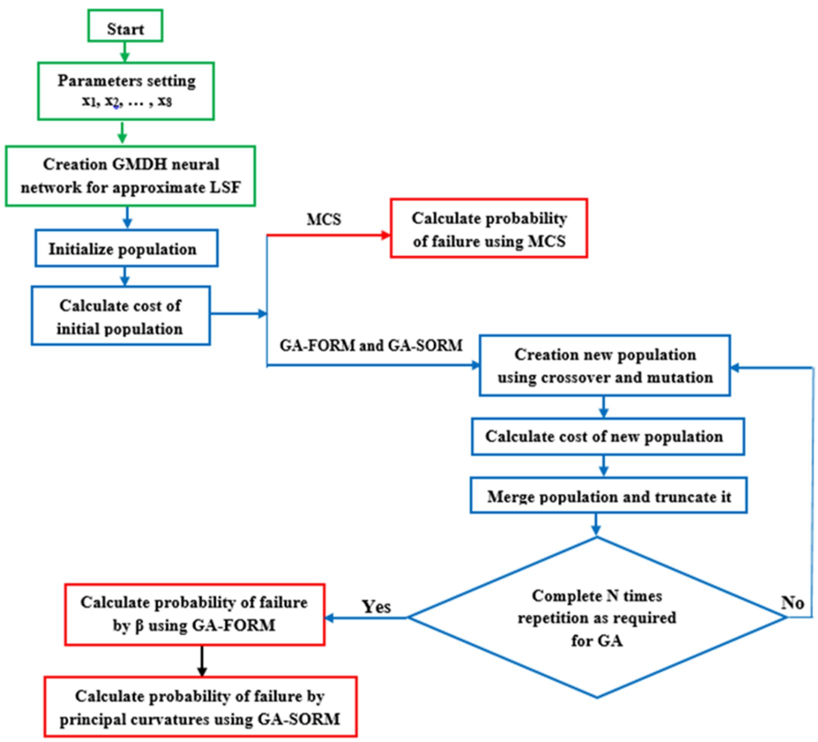


**Figure 9. Procedures of reliability analysis (suggested in this work).**

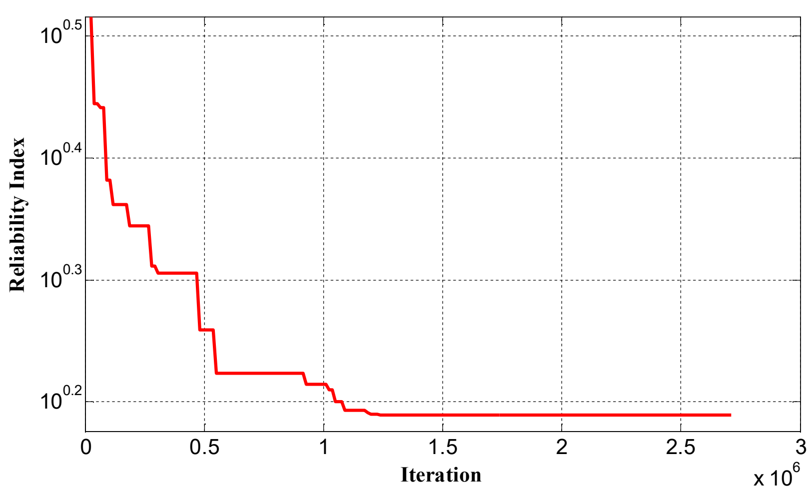


**Figure 10. Converge process of reliability index by GA.**

In the following, Table 8 presents the reliability index values with the corresponding PF values and the auxiliary terminology for the expected performance levels to illustrate the standard range of $\beta$ values [52]. According to the results of Table 5 and labels for the expected performance level in Table 8, the reliability indices of all points on the settlement surface is greater than 1.5, which satisfies the stability index required for a level II (unsatisfactory) that is specified in the "US army corps of engineers" standards. Therefore, in order to reduce the surface settlement, special arrangements must be made.

**Table 8 Labels for expected performance level of geo-technical works [52].**

| Reliability index $\beta$ | Probability of failure $P_F$ | Expected performance level |
|---|---|---|
| 1.0 | 0.16 | Hazardous |
| 1.5 | 0.07 | Unsatisfactory |
| 2.0 | 0.023 | Poor |
| 2.5 | 0.006 | Below average |
| 3.0 | 0.001 | Above average |
| 4.0 | 0.00003 | Good |
| 5.0 | 0.0000003 | High |

## 5. Conclusions

The main conclusions from this work could be mentioned as follow:

1. New time-invariant reliability methods were proposed by combining FORM, SORM, and MCS with GA and GMDH neural network for the reliability analysis of surface settlement caused by mechanized tunneling.

2. The most significant issue in SORM and FORM lies in finding the design point. In this work, GA was utilized for solving the problem of optimization (finding the design point using Eq. 11).

3. Choosing the LSF necessary for the reliability calculations in its closed-form is preferred. Unfortunately, the closed form often does not exist. In this work, the GMDH neural network was used to approximate LSF.

4. The average of the reliability index of the total settlement surface using MCS, GA-SORM, and GA- was obtained; GA-SORM and GA-FORM had a high calculation accuracy, and the calculation process was more concise than that of MCS.

5. The reliability index on each point of the model was calculated by the proposed reliability methods. The reliability degree of the tunnel could consequently be assessed at the local scale.

6. According to the "US army corps of engineers" standard, $\beta$ was >1.5, which satisfied the stability index required for a level II (unsatisfactory). Hence, special arrangements must be made to reduce the surface settlement.

## References

[1]. Hasanipanah. M., Noorian-Bidgoli. M., Armaghani. D.J., Khamesi. H. (2016). Feasibility of PSO-ANN model for predicting surface settlement caused by tunneling. Engineering with Computers 32 (4):705-715.

[2]. Fattahi H, Babanouri N. (2018). RES-Based Model in Evaluation of Surface Settlement Caused by EPB Shield Tunneling. Indian Geotechnical Journal:1-7.

[3]. Pourtaghi. A, Lotfollahi-Yaghin. M. (2012). Wavenet ability assessment in comparison to ANN for predicting the maximum surface settlement caused by tunneling. Tunnelling and Underground Space Technology 28:257-271.

[4]. Atkinson JH, Potts DM. (1977). Subsidence above shallow tunnels in soft ground. Journal of geotechnical and geoenvironmental engineering 103 (Proc. Paper 11318 Proceeding).

[5]. Hamza. M, Ata. A, Roussin. A. (1999). Ground movements due to the construction of cut-and-cover structures and slurry shield tunnel of the Cairo Metro. Tunnelling and Underground Space Technology 14 (3):281-289.

[6]. Chi S-Y, Chern J-C, Lin C-C. (2001). Optimized back-analysis for tunneling-induced ground movement using equivalent ground loss model. Tunnelling and Underground Space Technology 16 (3):159-165.

[7]. Chou. W-I, Bobet .A .(2002). Predictions of ground deformations in shallow tunnels in clay. Tunnelling and Underground Space Technology 17 (1):3-19.

[8]. Park K-H. (2005). Analytical solution for tunnelling-induced ground movement in clays. Tunnelling and Underground Space Technology 20 (3):249-261.

[9]. Ocak. I., Seker. S.E. (2013). Calculation of surface settlements caused by EPBM tunneling using artificial

neural network, SVM, and Gaussian processes. Environmental earth sciences 70 (3):1263-1276.

[10]. Mohammadi. S., Naseri. F., Alipoor. S. (2015). Development of artificial neural networks and multiple regression models for the NATM tunnelling-induced settlement in Niayesh subway tunnel, Tehran. Bulletin of engineering geology and the environment 74 (3):827-843.

[11]. Neaupane. K.M., Adhikari. N. (2006). Prediction of tunneling-induced ground movement with the multi-layer perceptron. Tunnelling and Underground Space Technology 21 (2):151-159.

[12]. Yao B-Z, Yang C-Y, Yao J-B, Sun. J. (2010). Tunnel surrounding rock displacement prediction using support vector machine. International Journal of Computational Intelligence Systems 3 (6):843-852.

[13]. Wang D-D, Qiu G-Q, Xie W-B, Wang Y. (2012). Deformation prediction model of surrounding rock based on GA-LSSVM-markov. Natural Science 4:1-6.

[14]. Santos Jr. O.J, Celestino. T.B. (2008). Artificial neural networks analysis of Sao Paulo subway tunnel settlement data. Tunnelling and Underground Space Technology 23 (5):481-491.

[15]. Suwansawat S, Einstein HH. (2006). Artificial neural networks for predicting the maximum surface settlement caused by EPB shield tunneling. Tunnelling and Underground Space Technology 21 (2):133-150.

[16]. Xu. J, Xu. Y. (2011). Grey correlation-hierarchical analysis for metro-caused settlement. Environmental earth sciences 64 (5):1249-1256.

[17]. Ercelebi S, Copur H, Ocak I. (2011). Surface settlement predictions for Istanbul Metro tunnels excavated by EPB-TBM. Environmental earth sciences 62 (2):357-365.

[18]. Zhao .H, Ru .Z, Chang .X, Yin .S, Li .S .(2014). Reliability analysis of tunnel using least square support vector machine. Tunnelling and Underground Space Technology 41:14-23.

[19]. Deng J, Gu D, Li X, Yue Z.Q. (2005). Structural reliability analysis for implicit performance functions using artificial neural network. Structural Safety 27 (1):25-48.

[20]. Elhewy A.H., Mesbahi. E, Pu Y. (2006). Reliability analysis of structures using neural network method. Probabilistic Engineering Mechanics 21 (1):44-53.

[21]. Cho S.E. (2009). Probabilistic stability analyses of slopes using the ANN-based response surface. Computers and Geotechnics 36 (5):787-797.

[22]. Lopes PAM, Gomes HM, Awruch AM. (2010). Reliability analysis of laminated composite structures using finite elements and neural networks. Composite Structures 92 (7):1603-1613.

[23]. Cheng J, Li Q. (2008). Reliability analysis of structures using artificial neural network based genetic algorithms. Computer Methods in Applied Mechanics and Engineering 197 (45-48):3742-3750.

[24]. Bauer J, Puła W. (2000). Reliability with respect to settlement limit-states of shallow foundations on linearly-deformable subsoil. Computers and Geotechnics 26 (3-4):281-308.

[25]. Rackwitz R, Flessler B. (1978). Structural reliability under combined random load sequences. Computers & structures 9 (5):489-494.

[26]. Cardoso J.B., De Almeida J.R., Dias J.M, Coelho P.G. (2008). Structural reliability analysis using Monte Carlo simulation and neural networks. Advances in Engineering Software 39 (6):505-513.

[27]. Breitung. K. (1984). Asymptotic approximations for multinormal integrals. Journal of engineering mechanics 110 (3):357-366.

[28]. Hurtado JE, Alvarez DA. (2010). An optimization method for learning statistical classifiers in structural reliability. Probabilistic Engineering Mechanics 25 (1):26-34.

[29]. You K, Park Y, Lee J.S .(2005). Risk analysis for determination of a tunnel support pattern. Tunnelling and Underground Space Technology 20 (5):479-486.

[30]. Morin MA, Ficarazzo F .(2006). Monte Carlo simulation as a tool to predict blasting fragmentation based on the Kuz–Ram model. Computers & Geosciences 32 (3):352-359.

[31]. Stroeve SH, Blom HAP, Bakker G (2009) Systemic accident risk assessment in air traffic by Monte Carlo simulation. Safety Science 47 (2):238-249.

[32]. Fattahi H, Shojaee S, Farsangi MAE, Mansouri H .(2013). Hybrid Monte Carlo simulation and ANFIS-subtractive clustering method for reliability analysis of the excavation damaged zone in underground spaces. Computers and Geotechnics 54:210-221.

[33]. Mahadevan S .(1997). Monte Carlo simulation. In: Cruse T (ed) Reliability-based mechanical design. Marcel Dekker, New York, pp 123-146

[34]. Holland J.H. (1975). Adaptation in natural and artificial systems: an introductory analysis with applications to biology, control, and artificial intelligence. U Michigan Press,

[35]. Chamkalani A, Mae'soumi A, Sameni A. (2013). An intelligent approach for optimal prediction of gas deviation factor using particle swarm optimization and genetic algorithm. Journal of Natural Gas Science and Engineering 14:132-143.

[36]. Tun YW, Pedroso DM, Scheuermann A, Williams DJ. (2016). Probabilistic reliability analysis of multiple slopes with genetic algorithms. Computers and Geotechnics 77 (1):68-76.

[37]. Zeng P, Jimenez R, Jurado-Piña R. (2015). System reliability analysis of layered soil slopes using fully specified slip surfaces and genetic algorithms. Engineering Geology 193:106-117.

[38]. Juang CH, Wang L. (2013). Reliability-based robust geotechnical design of spread foundations using multi-objective genetic algorithm. Computers and Geotechnics 48:96-106.

[39]. Ivakhnenko AG. (1971). Polynomial theory of complex systems. IEEE Transactions on systems, Man, and Cybernetics (4):364-378.

[40]. Naderpour H, Nagai K, Fakharian P, Haji M. (2019). Innovative models for prediction of compressive strength of FRP-confined circular reinforced concrete columns using soft computing methods. Composite Structures 215:69-84.

[41]. Fattahi H, Hasanipanah M, Zandy Ilghani N. (2021). Investigating Correlation of Physico-Mechanical Parameters and P-Wave Velocity of Rocks: A Comparative Intelligent Study. Journal of Mining and Environment 12 (3):863-875.

[42]. Mehrannia H, Pakgohar A. (2014). Using easy fit software for goodness of fit test and data generation. International Journal of Mathematical Archive 5 (1):118-124.

[43]. Fattahi H. (2017). Applying soft computing methods to predict the uniaxial compressive strength of rocks from schmidt hammer rebound values. Computational Geosciences 21 (4):665-681.

[44]. Fattahi H. (2020). A New Method for Forecasting Uniaxial Compressive Strength of Weak Rocks. Journal of Mining and Environment 11 (2):505-515.

[45]. Fattahi H, Babanouri N. (2017). Applying optimized support vector regression models for prediction of tunnel boring machine performance. Geotechnical and Geological Engineering 35 (5):2205-2217.

[46]. Fattahi H, Bazdar H. (2017). Applying improved artificial neural network models to evaluate drilling rate index. Tunnelling and Underground Space Technology 70:114-124.

[47]. Fattahi H, Moradi A. (2018). A new approach for estimation of the rock mass deformation modulus: a rock engineering systems-based model. Bulletin of engineering geology and the environment 77 (1):363-374.

[48]. Fattahi H. (2020). Analysis of rock mass boreability in mechanical tunneling using relevance vector regression optimized by dolphin echolocation algorithm. International Journal of Optimization in Civil Engineering 10 (3):481-492.

[49]. Fattahi H, Hasanipanah M An integrated approach of ANFIS-grasshopper optimization algorithm to approximate flyrock distance in mine blasting. Engineering with Computers:1-13.

[50]. Wang Y, Cao Z, Au S-K. (2010). Efficient Monte Carlo simulation of parameter sensitivity in probabilistic slope stability analysis. Computers and Geotechnics 37 (7):1015-1022.

[51]. Suchomel R, Mašı D. (2010). Comparison of different probabilistic methods for predicting stability of a slope in spatially variable c–φ soil. Computers and Geotechnics 37 (1-2):132-140.

[52]. Engineers UACo (1997). Engineering and design: Introduction to probability and reliability methods for use in geotechnical engineering. Engineer Technical Letter.

# آنالیز قابلیت اعتماد نشست سطح زمین ناشی از تونل‌سازی مکانیزه – مطالعه موردی

**هادی فتاحی[۱*] و فاطمه جیریایی[۲]**

**دانشکده مهندسی علوم زمین، دانشگاه صنعتی اراک، اراک، ایران**

ارسال۲۰۲۲/۰۱/۱۳ پذیرش ۲۰۲۲/۰۲/۲۰

* نویسنده مسئول مکاتبات: h.fattahi@arakut.ac.ir

**چکیده:**

نشست سطحی زمین، یک پارامتر مهم در عملیات تونل‌سازی مکانیزه است که باید قبل از حفاری مشخص شود. تجزیه و تحلیل نشست سطحی زمین ناشی از تونل‌سازی مکانیزه یک مسئله‌ی ژئوتکنیکی است که با منابع مختلف عدم قطعیت مشخص می‌شود. برخلاف روش‌های قطعی، تحلیل قابلیت اعتماد می‌تواند عدم قطعیت‌ها را برای ارزیابی نشست سطحی در نظر بگیرد. در این تحقیق، روش‌های آنالیز قابلیت اعتماد (روش قابلیت اعتماد مرتبه دوم (SORM)، شبیه‌سازی مونت کارلو (MCS) و روش قابلیت اعتماد مرتبه اول (FORM) بر مبنای الگوریتم ژنتیک (GA) برای ساخت مدل‌هایی برای تجزیه و تحلیل قابلیت اعتماد نشست سطحی به‌کار گرفته شد. از طرفی، برای روش‌های قابلیت اعتماد، تابع حالت حدی (LSF) غیر خطی است و برای استفاده از روش‌های قابلیت اعتماد مورد نیاز است. به منظور حل این مشکل، شبکه عصبی GMDH می‌تواند LSF را بدون نیاز به فرضیات اضافی در مورد شکل تابع تخمین بزند. در اینجا، شبکه عصبی GMDH برای به دست آوردن LSF بکار گرفته شده است. در شبکه عصبی GMDH، فشار تزریق انتهای چال، سطح آب زیرزمینی تونل، عمق، میانگین نرخ نفوذ، فاصله از چال، زاویه شیب، میانگین فشار جبهه‌کار و درصد پر شدن دوغاب به عنوان پارامترهای ورودی استفاده شده، در عین حال، نشست سطحی پارامتر خروجی می‌باشد. داده‌های میدانی متروی Bangkok به منظور نشان دادن توانایی روش‌های قابلیت اعتماد پیشنهادی، مورد استفاده قرار گرفته است.

**کلمات کلیدی:** نشست سطحی زمین، تونل‌سازی مکانیزه، روش‌های قابلیت اعتماد، شبکه عصبی GMDH، الگوریتم ژنتیک.